

RECORDS ADMINISTRATION



R0138976

DP -430 ✓

Metallurgy and Ceramics

Reactors - Power

AEC Research and Development Report

**FABRICATION OF  
URANIUM OXIDE FUEL ELEMENTS**

by

**G. R. Cole, A. S. Ferrara, and H. H. Kranzlein**

**Pile Materials Division**

**December 1959**

**RECORD  
COPY**

**DO NOT RELEASE  
FROM FILE**

**E. I. du Pont de Nemours & Co.  
Savannah River Laboratory  
Aiken, South Carolina**

This report was prepared as an account of Government sponsored work. Neither the United States, nor the Commission, nor any person acting on behalf of the Commission:

- A. Makes any warranty or representation, expressed or implied, with respect to the accuracy, completeness, or usefulness of the information contained in this report, or that the use of any information, apparatus, method, or process disclosed in this report may not infringe privately owned rights; or
- B. Assumes any liabilities with respect to the use of, or for damages resulting from the use of any information, apparatus, method, or process disclosed in this report.

As used in the above, "person acting on behalf of the Commission" includes any employee or contractor of the Commission, or employee of such contractor, to the extent that such employee or contractor of the Commission, or employee of such contractor prepares, disseminates, or provides access to, any information pursuant to his employment or contract with the Commission, or his employment with such contractor.

Printed in USA. Price \$1.00  
Available from the Office of Technical Services  
U. S. Department of Commerce  
Washington 25, D. C.

255239 ✓

DP - 430

METALLURGY AND CERAMICS  
REACTORS - POWER  
(TID-4500, 15th Ed.)

FABRICATION OF URANIUM OXIDE FUEL ELEMENTS

by

G. Rolland Cole, Anthony S. Ferrara, and Harvard H. Kranzlein

December 1959

E. I. du Pont de Nemours & Co.  
Explosives Department - Atomic Energy Division  
Technical Division - Savannah River Laboratory

Printed for  
The United States Atomic Energy Commission  
Contract AT(07-2)-1

Approved by  
P. H. Permar, Research Manager  
Pile Materials Division

#### ABSTRACT

Experimental fuel elements of  $\text{UO}_2$  clad in metallic sheaths were fabricated by swaging, rolling, and coextrusion. The effects of the type of  $\text{UO}_2$  and of the materials and dimensions of the sheath were investigated. Fused  $\text{UO}_2$  swaged in stainless steel tubing reached a maximum density of 93% of theoretical.

## CONTENTS

	<u>Page</u>
List of Figures	4
Introduction	5
Summary	5
Discussion	6
Background	6
Types of Uranium Oxide	7
Swaging of Rods	10
Fused UO <sub>2</sub>	12
Sintered PWR Pellets	13
PWR-Grade UO <sub>2</sub>	13
Steam-Oxidized UO <sub>2</sub>	15
Influence of Sheath Characteristics	17
Swaging of Tubes	22
Two-Die Swager	22
Four-Die Swager	23
Rolling of Rods	24
Rolling of Ribbons	27
Coextrusion of Rods	31
Bibliography	35

## LIST OF TABLES

<u>Table</u>		
I	Grades of Arc-Fused UO <sub>2</sub>	9
II	Density of Fused UO <sub>2</sub> after Swaging	9
III	Effect of UO <sub>2</sub> Particle Size on Density after Swaging	12
IV	Effect of Initial Density on Final Density and Sheath Thickness	13
V	Effect of Sheath Material on Density of Swaged UO <sub>2</sub>	17
VI	Effect of Wall Thickness on Density of Swaged UO <sub>2</sub>	19
VII	Density of UO <sub>2</sub> in Rolled Rods	24
VIII	Stratification in Flat-Rolled Specimens	30
IX	Density of UO <sub>2</sub> in Coextruded Rods	33

## LIST OF FIGURES

<u>Figure</u>	<u>Page</u>
1 Arc-Fused UO <sub>2</sub>	8
2 Grades of Fused UO <sub>2</sub>	8
3 Swaging Behavior of Rods - Fused UO <sub>2</sub>	11
4 Swaging Behavior of Rods - PWR-Grade UO <sub>2</sub>	11
5 Effect of Particle Size on Swaging Behavior of PWR-Grade UO <sub>2</sub>	14
6 Effect of Initial Density on Swaging Behavior of PWR-Grade UO <sub>2</sub>	14
7 Appearance of Cold-Swaged and Hot-Swaged PWR-Grade UO <sub>2</sub>	15
8 Effect of Oxide Type on Swaging Behavior of Rods	16
9 Effect of Initial Diameter on Swaging Behavior of UO <sub>2</sub> Rods	18
10 Effect of Initial Wall Thickness on Swaging Behavior of UO <sub>2</sub> Rods	18
11 Zircaloy-2-Clad Rod that Failed during Swaging	19
12 Zircaloy-2-Clad Rod Swaged to 50% Reduction in Area	20
13 Longitudinal Section of Permanent End Plug before Swaging	21
14 Permanent End Plug after Swaging	21
15 Swaged Tubular Element	23
16 Rolled Rod Elements	25
17 Sheath Failure of a Rolled Rod	25
18 Cross Sections of Swaged-and-Rolled Rods	26
19 Cross Section of Rolled Rod - Composite Sheath	26
20 Rolling Behavior of Ribbons - PWR-Grade UO <sub>2</sub>	27
21 Rolling Behavior of Ribbons - Fused UO <sub>2</sub>	28
22 Cross Sections of Rolled Ribbons	29
23 Effect of Rod Diameter on UO <sub>2</sub> Density in Rolled Ribbons	30
24 Twisted Ribbon Element	31
25 Coextrusion Billets	32
26 Typical Coextruded Rods	32
27 Radiographs of Coextruded Rods	33
28 Cross Section of Coextruded Rod	34

## FABRICATION OF URANIUM OXIDE FUEL ELEMENTS

### INTRODUCTION

The Savannah River Laboratory is developing oxide fuel elements for heavy-water-moderated power reactors fueled with natural uranium. Although metallic uranium is the first choice for the fuel material, it may have exposure limitations that make desirable the development of an oxide fuel element as a backup. The program is directed toward devising a fabrication process that is more attractive economically than the pressing and sintering process that is frequently used at the present time.

Fuel elements of  $UO_2$  can take various forms, but the simple rod form, or right circular cylinder, is the one most thoroughly proved and widely applied in power reactor service at present. The rod shape is resistant to deformation by internal pressure and is relatively easy to fabricate, but alternative shapes that have a higher surface-to-volume ratio, e.g., tubes and flat or twisted ribbons, may be more attractive if they can be produced cheaply and prove to be reliable in service.

There are a number of alternative processes for the fabrication of oxide fuel elements. Dense pellets of  $UO_2$  can be made by pressing, followed by high temperature sintering. The pellets are subsequently encased in a metal sheath to produce a fuel element. Swaging and rolling are processes that simultaneously densify the  $UO_2$  within a metal sheath and form the element to the final shape and size. Either swaging or rolling may produce clad fuel elements more economically than they can be produced by a pressing and sintering process.

This report summarizes the investigations at the Savannah River Laboratory from November 1957 to May 1959 on the fabrication of  $UO_2$  fuel elements by swaging, rolling, and coextrusion.

### SUMMARY

Rotary swaging of rods and tubes, rolling of rods and ribbons, and coextrusion of rods were investigated for the fabrication of  $UO_2$  fuel elements.

Swaged rods represent the most attractive fabrication method and shape at the present stage of development. The densities that can be produced with various types of core and sheath materials are well known, and little further development would be required to define a production process. The best results were obtained by swaging small diameter rods of arc-fused  $UO_2$  in stainless steel sheathing. Rods were swaged to densities up to 93% of theoretical, and the control of diameter and wall thickness was satisfactory.

Swaged tubes appear to be attractive, and most of the future work on this program will be concentrated on the swaging of tubular fuel elements. Oxide densities are comparable to those of rod elements. Techniques for removing the mandrel and for controlling the thickness of the annulus appear to be the next problems to be solved.

Roll forming produced rods and ribbons with  $UO_2$  densities from 86 to 88% of theoretical compared to 92% for swaged rods; the dimensions and shapes of the rolled specimens were poorly controlled. Problems remaining in the rod rolling process include sheath failure when wall thicknesses of practical interest are employed, and bowing of the rods. Improvement in the design of the roll grooves, and the addition of roll guides might solve these problems. The maximum  $UO_2$  densities in rolled ribbons were lower than those of swaged or rolled rods, primarily because of sheath springback at large area reductions.

Coextruded rods were made with fused  $UO_2$  cores and aluminum alloy sheaths. The rods, coextruded at about  $450^\circ C$ , had oxide densities substantially lower than those obtained by the other fabrication methods. It is anticipated that coextrusions at higher temperatures,  $800^\circ C$  and up, in suitable cladding materials would produce cores of higher densities.

For a given fabrication method and fuel shape the final  $UO_2$  density depended upon the type of  $UO_2$  used, the amount that the cross-sectional area was reduced in the fabrication process, and the nature of the sheath material. Variables such as specimen size and sheath thickness had minor effects.

## DISCUSSION

### BACKGROUND

Dimensional stability, resistance to coolant corrosion, high thermal conductivity, good nuclear reactivity, and low cost are characteristics desired in a power reactor fuel material. Contemporary  $UO_2$  fuel elements meet the first two requirements, but are somewhat lacking with respect to the remaining three. Extensive irradiation tests on sintered pellets of  $UO_2$  have shown that volume increases are negligible even at high burnup.<sup>(1,2)</sup> Uranium dioxide, having a cubic lattice, is isotropic and thus is not subject to the dimensional changes under thermal cycling or irradiation that have been exhibited by metallic uranium. Uranium dioxide is not attacked chemically by deoxygenated water at high temperature.<sup>(3,4)</sup> Dilution by oxygen atoms lowers the nuclear reactivity of uranium, but unenriched  $UO_2$  is usable if zirconium cladding and heavy water moderation are employed.<sup>(2)</sup> The thermal conductivity of  $UO_2$  is low, only one-third that of metallic uranium at ordinary temperatures, and it decreases with increasing temperature;<sup>(5-a)</sup> however, the low thermal conductivity of the oxide is partially compensated by its high melting point. To achieve low cost nuclear power there is need to lower the capital cost per unit of

installed power capacity and to reduce the fuel costs. The program discussed in this report was aimed primarily at the development of a low cost fuel element.

Uranium dioxide fuel elements made by encasing pressed and sintered pellets within metal tubing are generally accepted for power reactor use. Their reliability has been demonstrated in the Westinghouse pressurized water reactor (PWR) and in the Vallecitos boiling water reactor of the General Electric Company (VBWR); oxide fuel elements are specified for several reactors not yet in operation (the Dresden reactor, the Nuclear Power Demonstration reactor, and the Nuclear Ship Savannah reactor, for example).

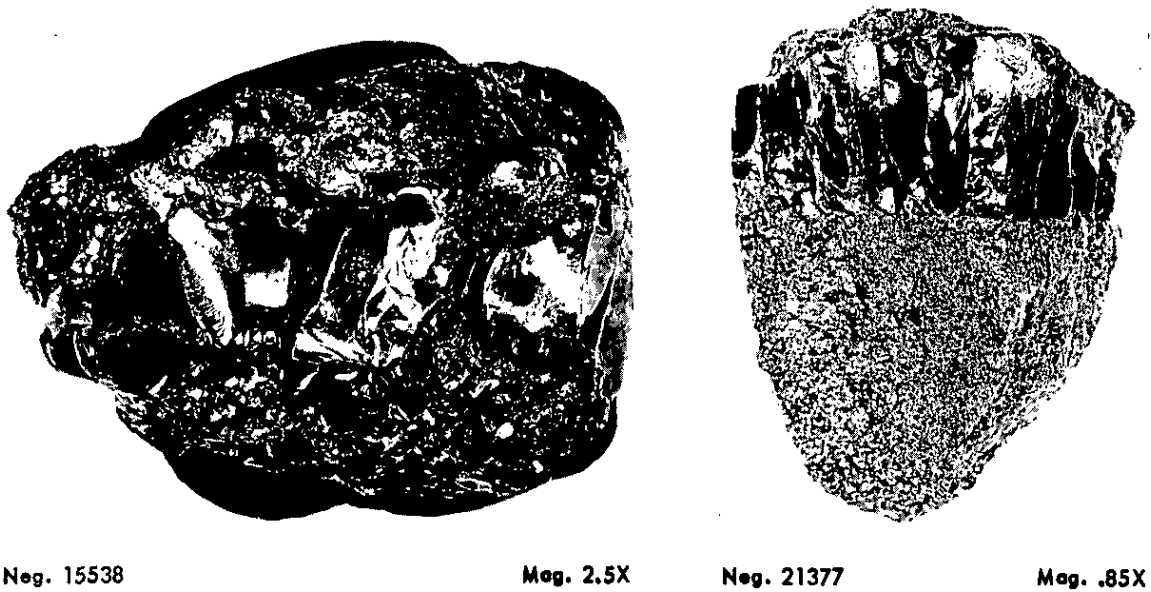
Fabrication methods that densify the  $UO_2$  and form the clad fuel element in one operation, such as swaging and rolling, are potentially low cost processes; a proven process, together with a reliable cost estimate, is not yet available, however. Swage fabrication of  $UO_2$  fuel rods has been investigated at the Hanford Atomic Products Operation<sup>(9)</sup>, at Chalk River<sup>(10)</sup>, and at the Savannah River Laboratory.

High bulk density is a desirable feature in unenriched  $UO_2$  fuel. It is probably the most important single index of  $UO_2$  fuel quality and, as such, receives considerable attention in this report. Nuclear reactivity can be increased by maximizing the density, or the number of uranium atoms per unit volume. High density oxide, in which the number of pores or voids is low, has greater thermal conductivity. Postirradiation studies have shown that release of fission product gases, which can cause pressure buildup in the element or progressive decrease in heat transfer capability, increases with decreasing  $UO_2$  density.<sup>(1,2)</sup>

## TYPES OF URANIUM OXIDE

The highest swaged densities observed in this investigation were obtained with arc-fused  $UO_2$ . This  $UO_2$  was fused at the Chippawa, Ontario, Plant of the Norton Company by a method similar to that commonly employed to fuse alumina or magnesia. The two lots of product received consisted mostly of irregular chunks ranging in size from 1/2 to 3 inches in the greatest linear dimension.

The fused  $UO_2$  varied in quality from piece to piece, and some of the larger chunks varied in quality within a single piece. For example, two pieces containing large, shiny crystals adjacent to regions of rough material are shown in Figure 1. After the  $UO_2$  chunks were crushed into smaller pieces, they were graded by appearance. Typical graded pieces are shown in Figure 2; a brief description of each grade is given in Table I.



Neg. 15538

Mag. 2.5X

Neg. 21377

Mag. .85X

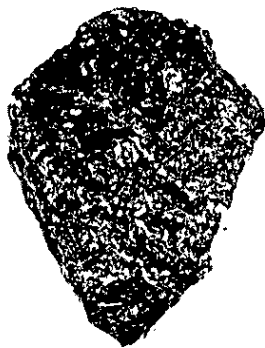
FIGURE 1 - ARC - FUSED  $UO_2$



Neg. 21837 Mag. .85X  
Grade 1.



Neg. 21845 Mag. 1.3X  
Grade 2+



Neg. 21838  
Grade 2



Mag. .85X  
Grade 2-



Neg. 21837 Mag. .85X  
Grade 5

FIGURE 2 - GRADES OF FUSED  $UO_2$

TABLE I

Grades of Arc-Fused UO<sub>2</sub>

Grade Number	Appearance	Representative Chunk Density, % of theoretical	Oxygen-to-Uranium Ratio	
			Lot 1 <sup>(a)</sup>	Lot 2 <sup>(b)</sup>
1	Smooth and shiny, with good crystal faces	100	2.058	2.047
1"Select"			2.014	-
2+	Smooth, but not so shiny	98	2.142	2.096
2	Rough surfaces	95	2.145	2.063
2-	Rough, dull surfaces	86	2.192	2.039
3	Crushing fines (a mixture of the other grades)	-	2.193	-
4	Powder at the bottom of the shipping container	-	2.206	-
5	Shiny, but with surface craters	93	-	2.113
Average		-	2.14	2.08

(a) Lot 1 consisted of a single fusion, 300 lb of product.

(b) Lot 2 consisted of a series of 26 fusions, 16,800 lb of product. The evaluation of Lot 2 is not yet complete.

TABLE II

Density of Fused UO<sub>2</sub> after Swaging

Minus 20-mesh UO<sub>2</sub> in stainless steel cladding  
 Initial diameter = 5/8 inch  
 Initial wall thickness = 0.035 inch  
 UO<sub>2</sub> area reduction = 49%

UO <sub>2</sub> Grade (described in Table I)	1	2+	2	2-	3	4	5
UO <sub>2</sub> Density, % of theoretical	92	91	92	91	92	85	91

Much of the fused oxide contained excess oxygen. Analyses, summarized in Table I, showed ratios of oxygen to uranium that ranged from 2.00 to 2.25 (corresponding to  $UO_{2.00}$  and  $UO_{2.25}$ ). The theoretical, or X-ray, density of uranium oxide increases from 10.97 to 11.3 as the O/U ratio increases from 2.00 to 2.25.<sup>(1)</sup> The variations involved are relatively small, and for convenience all fabricated oxide densities are reported in terms of "per cent of theoretical" and are based on the theoretical density of stoichiometric  $UO_2$  ( $10.97 \text{ g/cm}^3$ ). Excess oxygen is thought to impair the in-pile performance of the fuel elements,<sup>(2)</sup> but should have little effect on the results of fabrication studies at ordinary temperatures.

The carbon and iron contents of samples ranged from <50 to 200 ppm and from zero to 700 ppm, respectively. Carbon, present as UC or  $UC_2$ , is susceptible to attack by hot water, and thus impairs the over-all corrosion resistance. Iron is a neutron absorber and therefore is an undesirable impurity.

Other types of uranium oxide were investigated.

PWR-grade powder Produced by the reduction of  $UO_3$ . The material was supplied by the Uranium Division of the Mallinckrodt Chemical Works.

Sintered pellets Reject pellets from the Bettis Plant production for the PWR. The pellets had a sintered density of about 93% of theoretical and were crushed to pass a 20-mesh sieve before swaging.

Steam-oxidized uranium Produced by oxidation of uranium metal in steam at a pressure of 125 psi and a temperature of  $170^\circ\text{C}$ . The product was a fluffy powder with an O/U = 2.19.

#### SWAGING OF RODS

Most of the experimental effort was concentrated on swaged rods, and higher  $UO_2$  densities and better control were achieved with the swaged rod elements than with other fabrication methods and fuel shapes. For example,  $UO_2$  densities up to 93% of theoretical were obtained by swaging fused  $UO_2$  through an area reduction of 50%; the stainless steel sheathing was 0.035 inch thick and 0.625 inch in diameter initially. One series of six similar rods, with fused  $UO_2$  in 0.0325-inch-thick stainless steel, was swaged from 0.750-inch initial diameter to 0.575-inch final diameter with the following results and ranges: final diameter =  $0.575 \pm 0.002$  inch, sheath thickness =  $0.0325 \pm 0.001$  inch, and  $UO_2$  density =  $90.8 \pm 0.8\%$  of theoretical.

Rod shapes were made by loading  $UO_2$  into metal tubing, after which the cross-sectional area was reduced by swaging. In most cases the  $UO_2$  powder was contained in the tubing by rubber end plugs. Specimen diameter, or cross-sectional area, was reduced by passes through progressively smaller dies in the swaging machine. The area reduction of a specimen is defined by the formula

Area reduction =  $(\text{Initial area} - \text{Final area}) / (\text{Initial area})$

Most of the swaging experiments were performed with a two-die swaging machine, Fenn Model 6F. A few experiments were performed with a Fenn Model 4F swaging machine of the four-die type.

The reduction in cross-sectional area of the rod\* densified the UO<sub>2</sub>, changed the thickness of the metal sheath, and elongated the rod. Figure 3 shows these changes as functions of area reduction for fused UO<sub>2</sub>. At small area reductions the UO<sub>2</sub> densified easily; the UO<sub>2</sub> provided little support for the metal sheath, which increased in thickness without elongation as an empty tube does during swaging. At area reductions between 20 and 40%, the UO<sub>2</sub> became more dense and began to resist further reduction, thinning the sheath and causing the rod to elongate. For fused UO<sub>2</sub>, a maximum density was reached at an area reduction of about 40%. Further reduction served only to elongate the rod and to thin the sheath at an increased rate. The comparable behavior for PWR-grade UO<sub>2</sub> (shown in Figure 4) differs from the fused oxide in that the density continued to rise at area reductions above 40%. The area reduction for both cases was limited to 68% by the range of die sizes available.

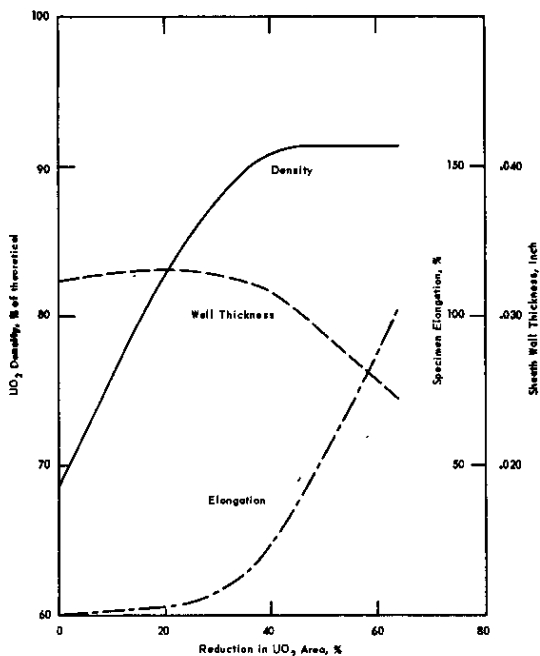


FIGURE 3 - SWAGING BEHAVIOR OF RODS - FUSED UO<sub>2</sub>

Type 316 Stainless Steel Sheath;  
Initial Rod Diameter = 0.750 inch,  
Wall Thickness = 0.0325 inch

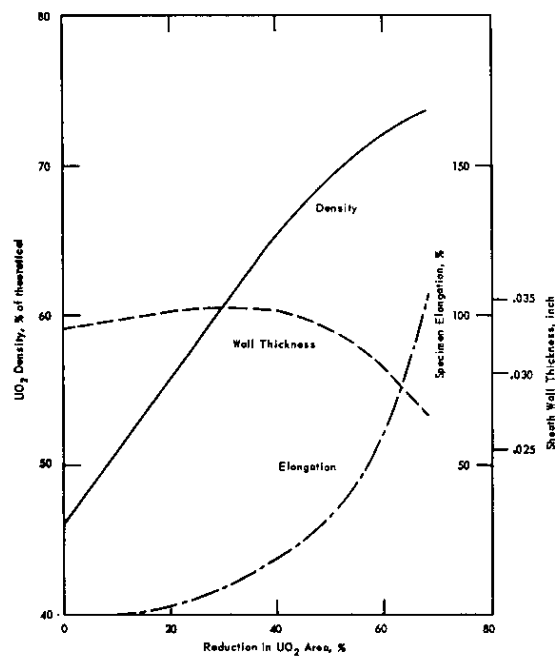


FIGURE 4 - SWAGING BEHAVIOR OF RODS - PWR-GRADE UO<sub>2</sub>

Type 316 Stainless Steel Sheath;  
Initial Rod Diameter = 0.750 inch,  
Wall Thickness = 0.033 inch

\*The word that describes the shape, e.g., rod, refers to the UO<sub>2</sub> itself. The oxide is always contained within a metal tube when fabricated by this means.

The density obtained for a given reduction in area depended greatly on the type of uranium oxide. Fused UO<sub>2</sub> reached the highest maximum density, 93% of theoretical, followed by crushed, sintered pellets with 89%, steam-oxidized material with 80%, and PWR-grade oxide with 75%.

#### FUSED UO<sub>2</sub>

The various "grades" of fused UO<sub>2</sub>, with the exception of Grade 4, could be swaged to approximately equal densities despite the fact that the initial as-fused densities of the individual chunks varied from grade to grade (compare Tables I and II, page 9). The initial differences in density caused by the presence of macroscopic holes in some of the chunks were minimized by the pulverizing and swaging operations, which reduced the chunks to particles of 0.03 inch or less in size. Grade 4 was the designation for the oxide fines that lay on the bottom of the shipping drum in the form of powder.

The particle size to which the fused UO<sub>2</sub> was pulverized influenced the swaged density only slightly. The fused UO<sub>2</sub> was quite friable, so the larger particles fractured easily to give efficient packing during swaging. The swaged densities were slightly lower when the maximum particle size was less than 70 mesh. The data are listed in Table III. The density results are for a complete range of particle sizes in each case, with only the maximum particle size being specified. The pass-fractions were employed instead of specific cuts because the results have greater practical significance. Extensive sieve sizing and recycling of rejected fractions would be costly in production.

TABLE III

#### Effect of UO<sub>2</sub> Particle Size on Density after Swaging

Grade No. 2, fused UO<sub>2</sub> in stainless steel sheathing, Type 316  
 Initial diameter = 5/8 inch  
 Initial wall thickness = 0.035 inch  
 UO<sub>2</sub> area reduction = 52%  
 There was a range of particle sizes in each case; only the maximum particle size is specified.

<u>Sieve Size,</u> <u>mesh</u>	<u>Size of Largest</u> <u>Particle, inch</u>	<u>UO<sub>2</sub> Density,</u> <u>% of theoretical</u>
-6	0.132	91.6
-10	0.0787	91.6
-12	0.0661	91.3
-16	0.0469	91.8
-20	0.0331	91.6
-40	0.0165	91.5
-70	0.0083	90.8
-120	0.0049	90.2

The influence of initial packed density on final swaged density was minimized by moderate overswaging, but the constancy of final density was partially offset by variations in final sheath thickness; the applicable data for fused UO<sub>2</sub> are shown in Table IV.

TABLE IV

Effect of Initial Density on Final Density  
and Sheath Thickness

Grade No. 2 fused UO<sub>2</sub> crushed to minus 20 mesh  
Stainless steel sheath, initially 5/8 inch in diameter and  
0.035 inch thick  
UO<sub>2</sub> area reduction = 52 to 54%

UO <sub>2</sub> Density, % of theoretical		Final Sheath Thickness, inch
Initial	Final	
61.2	92.8	0.0314
64.2	93.0	0.0309
66.6	92.8	0.0303
70.5	92.7	0.0293

SINTERED PWR PELLETS

Relatively little swaging was performed with sintered and crushed PWR pellets. A density of 89% of theoretical was obtained with sintered pellets crushed to pass 20 mesh and contained in Type 316 stainless steel tubing. The rod diameter was reduced from 0.625 to 0.44 inch, while the wall thickness diminished from 0.035 to 0.031 inch.

PWR-GRADE UO<sub>2</sub>

The PWR-grade UO<sub>2</sub> had swaging characteristics similar to the fused UO<sub>2</sub> with two exceptions: the maximum density obtained was much lower, 75% compared with 93% of theoretical, and the density continued to increase slightly even at the highest area reduction attained.

The effects of particle-size distribution on initial packed density, swaged density, and sheath thickness for PWR-grade UO<sub>2</sub> in stainless steel are shown in Figure 5. PWR-grade UO<sub>2</sub> was separated into -200-mesh and +200-mesh fractions, and the swaging behaviors of the fractions were compared with that of the as-received powder. The packing and swaging characteristics of the -200-mesh fraction were very similar to those of the as-received oxide, but the +200-mesh oxide packed and swaged to lower densities. Superficially, this appears to be a reversal of the effect observed for the fused UO<sub>2</sub>, Table III, where the smaller particle sizes swaged less well, but there were important differences in the average size, brittleness, and toughness of the particles concerned. A wide distribution of particle sizes was present in the as-received and the -200-mesh samples, while the +200 mesh, which normally made up about 35% of the PWR-grade powder, densified less well because of its limited distribution of particle sizes. Furthermore, the PWR-grade

oxide particles were too small and tough (for their size) to overcome an unfavorable size distribution by fracturing and fitting together as did the fused  $UO_2$ .

It might appear that the difference in swaged density between the +200 mesh and the as-received PWR-grade  $UO_2$  could be explained solely by the difference in initial packing density, but the effect of initial density alone was not sufficient to account for the difference in final swaged density shown in Figure 5. Specimens containing identical samples of  $UO_2$ , deliberately packed to different initial densities, reached essentially equal final densities when swaged through a 60% area reduction, as shown in Figure 6.

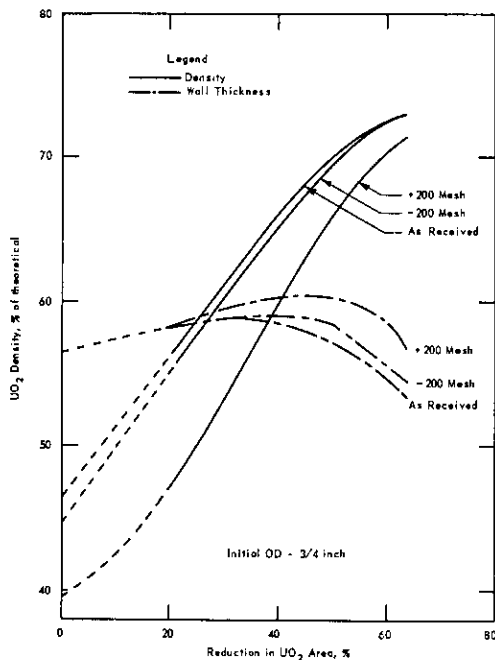


FIGURE 5 - EFFECT OF PARTICLE SIZE ON SWAGING BEHAVIOR OF PWR-GRADE  $UO_2$  Rods Sheathed in Type 316 Stainless Steel

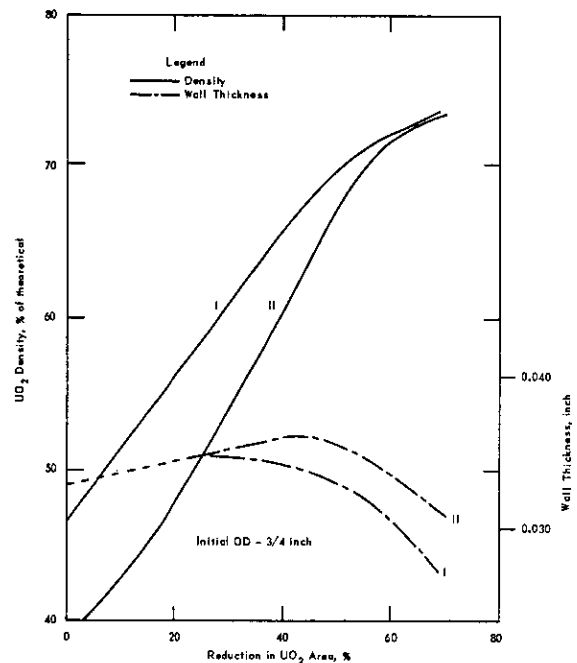
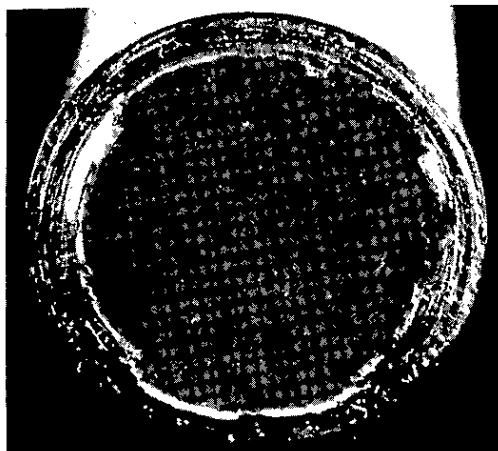


FIGURE 6 - EFFECT OF INITIAL DENSITY ON SWAGING BEHAVIOR OF PWR-GRADE  $UO_2$  PWR-Grade  $UO_2$  Rods Sheathed in Type 316 Stainless Steel

PWR-grade  $UO_2$  swaged to a greater density at high temperature than it did at room temperature, but still it was less dense than fused  $UO_2$  swaged at room temperature. The PWR-grade  $UO_2$ , loaded in 0.065-inch-wall stainless steel tubing, was swage-reduced from 0.750-inch diameter to 0.533 or 0.500 inch at room temperature and then was reduced in two passes to 0.435-inch diameter at a nominal temperature of 600°C. The true temperature was below the nominal temperature because approximately 30 seconds elapsed between the removal of the piece from the furnace and the swaging operation. The final  $UO_2$  densities were approximately 80% of theoretical for the pieces swaged hot, compared to a density of 75% of theoretical reached by similar specimens swaged at room temperature. Higher densities have been obtained with hot-swaged specimens of smaller diameter at the Hanford

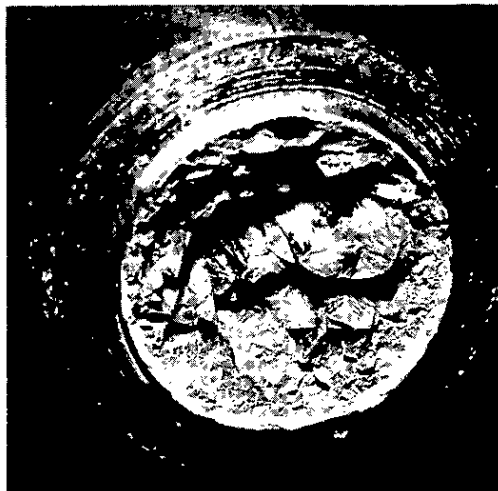
Laboratories.<sup>(12)</sup> Local variations in sheath wall thickness were apparent after hot swaging. The sheaths ruptured when specimens with 0.035-inch stainless steel cladding were hot swaged. The hot-swaged  $UO_2$  had a more coherent, harder appearance than did cold-swaged  $UO_2$  (see the comparison in Figure 7). Although the swaging temperature of  $600^\circ C$  was far below that appropriate for sintering, about  $1600^\circ C$ , the combination of high temperature and high swaging pressures may have produced an effect akin to sintering. Effective densification was achieved by a similar combination of less-than-sintering temperature and high pressure in hot pressing experiments.<sup>(13)</sup>



Neg. 21846

Mag. 5.7X

a. Swaged at Room Temperature



Neg. 17053

Mag. 5.7X

b. Swaged at a Nominal Temperature of  $600^\circ C$

FIGURE 7 - APPEARANCE OF COLD-SWAGED AND HOT-SWAGED PWR-GRADE  $UO_2$

## STEAM-OXIDIZED UO<sub>2</sub>

The change in density and the thickening of the sheath during swaging were relatively greater for the steam-oxidized UO<sub>2</sub> than for the other oxides investigated. The swaging behaviors of steam-oxidized and PWR-grade UO<sub>2</sub> are compared in Figure 8. Steam-oxidized UO<sub>2</sub> packed to a lower density and swaged to a higher density than did PWR-grade oxide. The important difference lies in the nature of the individual particles. Uranium oxide produced by the steam oxidation of uranium metal consists of comparatively dense platelets<sup>(14)</sup> that pack inefficiently, but break up readily and pack tightly under the vibration and pressure of swaging. This behavior is in marked contrast to that of the PWR-grade UO<sub>2</sub>, which has individual particles that are more regular in over-all shape, but less dense than the steam-oxidized material.

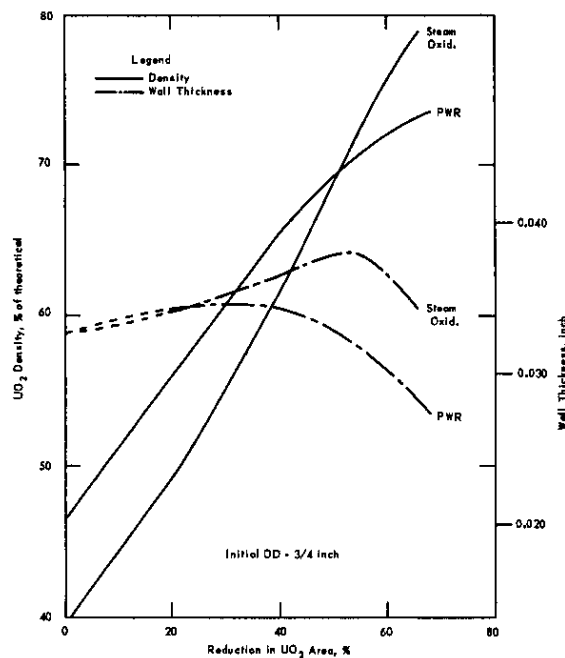


FIGURE 8 - EFFECT OF OXIDE TYPE ON SWAGING BEHAVIOR OF RODS

UO<sub>2</sub> Rods Sheathed in Type 316 Stainless Steel

INFLUENCE OF SHEATH CHARACTERISTICS

Higher swaged densities were reached with uranium oxide in stainless steel or Zircaloy-2 sheaths than in aluminum or carbon steel sheaths. Presumably, the sheath materials with the higher yield strengths flowed less readily and thus maintained a higher maximum pressure on the UO<sub>2</sub> during swaging. High area reductions were not obtained with the aluminum sheathing material because it split after a few passes through the swager. Table V compares the densities obtained with fused oxide and PWR-grade oxide in the various sheath materials.

TABLE V

Effect of Sheath Material  
on Density of Swaged UO<sub>2</sub>

Initial rod diameters = 3/4 inch  
 Initial wall thicknesses = 0.033 inch for stainless steel  
 0.022 inch for Zircaloy-2  
 0.065 inch for carbon steel  
 0.035 inch for aluminum

<u>Core Material</u>	<u>Sheath Material</u>	<u>UO<sub>2</sub> Area Reduction, %</u>	<u>UO<sub>2</sub> Density, % of theoretical</u>	<u>Comparable UO<sub>2</sub> Density in Stain- less Steel</u>
Fused UO <sub>2</sub> (-20 mesh)	Stainless Steel, Type 316	50	91.5	-
	Zircaloy-2	44	91.5	91.5
	Aluminum, Type 6063	49	87.5	91.5
PWR-grade UO <sub>2</sub> (as-received)	Stainless Steel, Type 316	68	74	-
	Zircaloy-2	42.5	64.5	66.5
	Carbon Steel	71	71	74

Sheath dimensions, e.g., initial diameter and thickness, had a slight influence on the final  $UO_2$  density. Oxide density after swaging was slightly lower for the larger initial diameters. Figure 9 shows this effect for both fused  $UO_2$  and PWR-grade  $UO_2$ . The data do not extend to the same maximum reductions for the different diameters because the extent of diameter reduction was limited by the size range of the swaging dies. For fused  $UO_2$  swaged in stainless steel, there was a difference of about 1% of theoretical density between specimens of 0.032- and 0.007-inch wall (Table VI). The density results for PWR-grade  $UO_2$  in 0.022- and 0.033-inch sheaths were essentially indistinguishable, while 0.066-inch wall specimens reached a density about 1% higher (Figure 10). The diameter effect was more important than the wall thickness effect. For example, in Figure 9, a comparison of results at an area reduction of 68% shows a density decrease of 2% of theoretical for a 33% larger initial diameter, but Figure 10 indicates a density decrease of only about 1% of theoretical for a 50% decrease in initial wall thickness. These data indicate that the influence of sheath dimensions on density is not simply a matter of diameter-to-wall-thickness ratio.

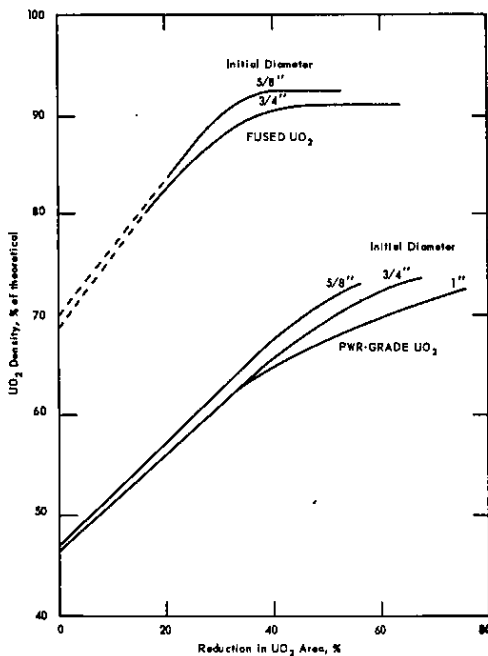


FIGURE 9 - EFFECT OF INITIAL DIAMETER ON SWAGING BEHAVIOR OF  $UO_2$  RODS  
 $UO_2$  Sheathed in Type 316 Stainless Steel

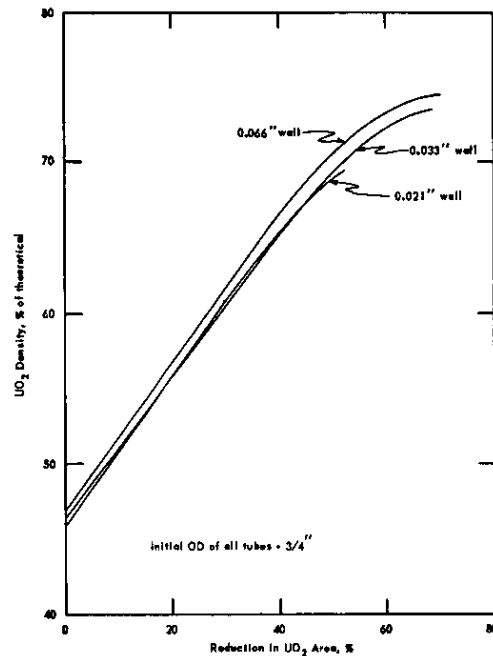


FIGURE 10 - EFFECT OF INITIAL WALL THICKNESS ON SWAGING BEHAVIOR OF  $UO_2$  RODS  
PWR - Grade  $UO_2$  Sheathed in Type 316 Stainless Steel

TABLE VI

Effect of Wall Thickness on Density of Swaged UO<sub>2</sub>

Initial diameters = 5/8 inch  
 Area reduction = 37 to 40%  
 Stainless steel type = 316 for 0.032-inch sheaths  
 304 for 0.020-, 0.014-, and 0.007-inch sheaths  
 Oxide = arc-fused

<u>Sheath Thickness,</u> <u>inch</u>	<u>UO<sub>2</sub> Density,</u> <u>% of theoretical</u>
0.032	91.2
0.020	90.8
0.014	90.4
0.007	90.5

Wrinkling at the ends of the specimens sometimes occurred with thin sheaths, but proper choice of end plug material or improved design minimized such wrinkling. This behavior was particularly troublesome with sheaths of 0.022-inch Zircaloy-2 and 0.014- and 0.007-inch stainless steel. Replacing the customary rubber end plugs with a mixture of rubber cement and iron filings or sand greatly reduced the sheath wrinkling. This composition end plug material was loaded to the end of the specimen to provide sheath support.

A failed Zircaloy-2 sheath is shown in Figure 11.

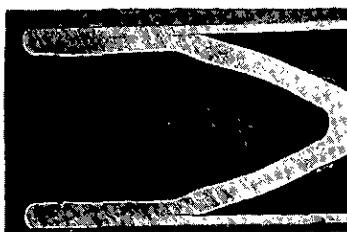


Neg. 16757

Actual Size

FIGURE 11 - ZIRCALOY-2-CLAD ROD THAT FAILED DURING SWAGING

The  $UO_2$  was contained in the specimen by rubber end plugs that left about 2 inches of sheath unsupported at each end of the specimen. Similar end closures with stainless steel cladding of 0.035-inch thickness were entirely satisfactory, but the 0.022-inch-thick Zircaloy-2 cladding cracked over the unsupported region. The crack started at the open end, crossed the rubber end plug, and reached the  $UO_2$ , terminating the experiment. Properly designed metal end plugs, welded flush with the specimen ends, provided sufficient sheath support to permit swaging through a core area reduction of 50%. The proper end plug design was achieved by making the metal end plugs strong enough to provide support for the sheath and to contain the  $UO_2$ , but weak enough to be reduced in diameter without cutting through the sheath. A sample is shown in Figure 12.



Neg. 18907                      Mag. 1.9X

a. Lengthwise Section at End Plug



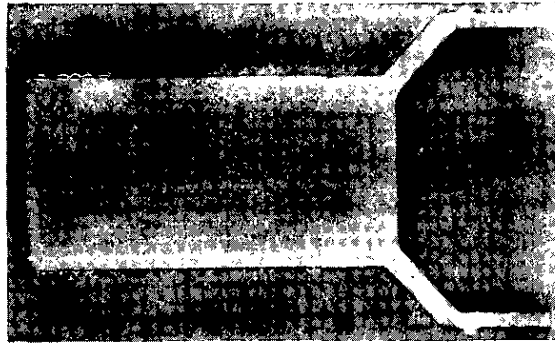
Neg. 18806

Mag. 2.5X

b. Exterior View at the Rod End

FIGURE 12 - ZIRCALLOY-2-CLAD ROD SWAGED TO 50% REDUCTION IN AREA

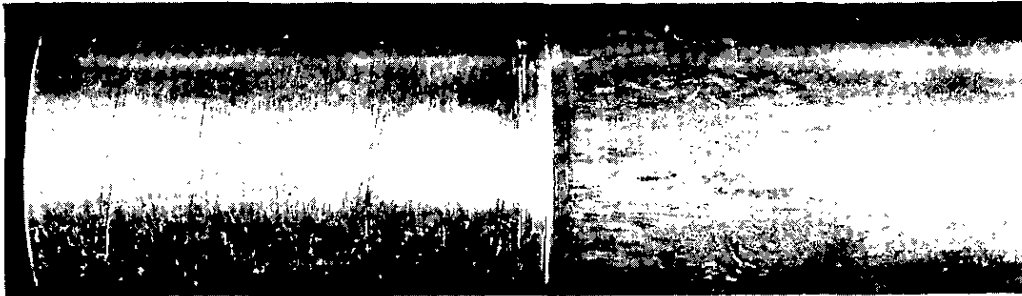
In the production of fuel rods, permanent end plugs would be economically preferable to temporary plugs that had to be replaced after swaging. A cross section of a promising design of permanent end plug is shown in Figure 13. The solid cylindrical portion can be made to form a special end fitting if desired. The ridge on the outside of the hollow portion is for alignment and welding purposes; the sheath butts against the ridge and is fusion welded to the ridge by the standard "Heliarc" technique. Exterior and sectional views of the end plug after swaging are shown in Figure 14. This type of end plug was satisfactory for stainless steel claddings as thin as 0.007 inch and for 0.022-inch Zircaloy cladding.



Neg. 18859

Mag. 2.3X

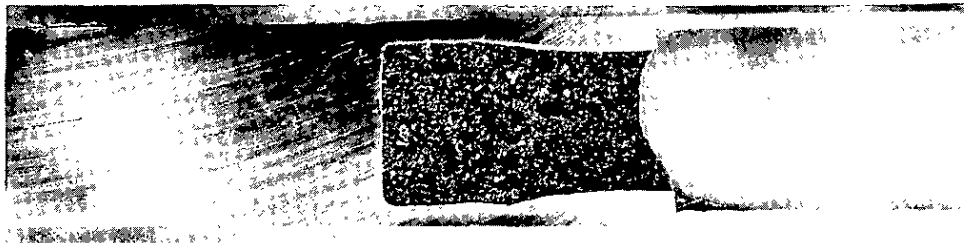
FIGURE 13 - LONGITUDINAL SECTION OF PERMANENT END PLUG BEFORE SWAGING



Neg. 18805

Mag. 3.4X

a. External Appearance, As - Swaged



Neg. 18826

Mag. 2.5X

b. Longitudinal Section



Neg. 18828

Mag. 2.5X

c. Longitudinal section etched to bring out the weld zone

FIGURE 14 - PERMANENT END PLUG AFTER SWAGING

## SWAGING OF TUBES

### TWO-DIE SWAGER

In preliminary experiments with a two-die swager, Fenn Model 6F, large diameter tubular elements were swaged to uranium oxide densities comparable to rod densities at intermediate area reductions. Swaging was limited to intermediate area reductions, approximately 30%, because the two-die swager became very difficult to feed at higher reductions. In order to develop the techniques without contaminating the equipment, much of the swaging of tube shapes was done with cores of sand, alumina or a mixture thereof, and only a few tubes containing uranium oxide were swaged.

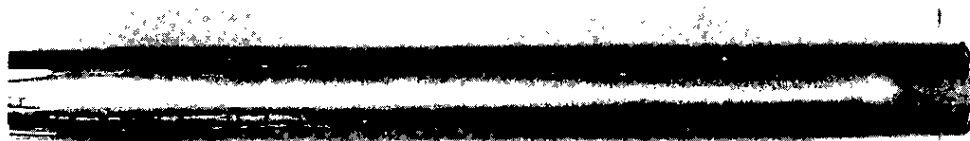
A tubular element, consisting of PWR-grade  $UO_2$  contained in an annulus between 0.022-inch-wall stainless steel tubes of 2.80- and 2.00-inch diameter, was swaged through an area reduction of 32% to give a density of 61.5% of theoretical. This was essentially the same as the density obtained when a 3/4-inch rod specimen was swaged to the same area reduction, as can be seen by reference to Figure 4. The sheath wall thickness, which was initially 0.021 inch, increased to 0.023 inch for the outer sheath, but was unchanged for the inner sheath, which was supported by the mandrel. The sheath behavior was in accord with expectations. The outer sheath thickened because it was being reduced in diameter with very little accompanying elongation; up to this reduction, the uranium oxide was still densifying without much resistance.

A similar tubular element containing fused uranium oxide pulverized to pass a 20-mesh screen was swaged through an area reduction of 30% to an oxide density of 85% of theoretical. This density is 3% lower than that obtained by swaging a 3/4-inch rod specimen through the same area reduction. The wall thickness behavior indicated that the specimen was farther along in the swaging pattern than was the PWR-grade tubular specimen. The outer sheath was 0.021 inch thick; presumably it had already thickened, and was now beginning to thin. The inner sheath was 0.020 inch thick; the oxide had begun to resist further densification and was working the inner sheath slightly, as well as forcing the outer sheath to elongate.

Two views of a swaged tube are shown in Figure 15. The wrinkling of the unsupported sheath is apparent at the ends, as is a crack over the rubber end plug.

The inside diameter of each tube was supported by one of two types of mandrels: (1) an "anchored" mandrel that was fixed between the swaging dies but free to rotate, or (2) a "traveling" mandrel that moved with the tube. The traveling mandrels gave better results than the anchored mandrels. Tubes swaged using the anchored mandrel system were characterized by wrinkles in the inner sheath and occasional ovality of

the outer sheath. The traveling mandrel system produced a better surface on the inner sheath, but the mandrel was difficult to remove from the tube after swaging. Temporary end plugs of rubber or composition material were used; metal end plugs welded in place would have failed because of the unequal elongations of the inner and outer sheaths. End plugs of cast lead proved unsatisfactory.



Neg. 20510

Mag. 0.2X



Neg. 20509

Mag. 0.2X

**FIGURE 15 - SWAGED TUBULAR ELEMENT**  
The sheath wrinkled at the ends, which were not supported by core material. The bottom view shows a crack over the rubber end plug.

#### FOUR-DIE SWAGER

As the next step in the development program, tubular elements loaded with sand and aluminum oxide were swaged in a four-die swager at the Penn Company Plant in Newington, Connecticut. These tubes were reduced from 2.500 to 2.060 inches in outside diameter in 14 passes, while the inside diameter, a nominal 1.460 inches, was supported by a hollow steel traveling mandrel. The sheath material was Type 304 stainless steel, 0.022 inch thick.

The four-die swaging machine was superior to the two-die machine from the standpoints of ease of feeding the tube into the dies and of final surface quality of the sheaths. An area reduction of 52% was obtained with the four-die swager, compared with the maximum area reduction of 32% reached with the two-die swager.

Because of its obvious operating advantages, the four-die swager was adopted as the principal tool for the fabrication of tubular oxide fuel elements. An extensive development program for the swaging of fused  $UO_2$  is underway and will be described in future reports.

## ROLLING OF RODS

The general pattern of loading, handling, and density behavior for a rolled rod was similar to that of a swaged rod. The rods were passed through grooved rolls of 16-inch diameter at a speed of approximately 15 ft/min. The roll parting was 0.063 inch. The maximum densities obtained were slightly higher for PWR-grade UO<sub>2</sub> specimens and slightly lower for fused oxide specimens than were the densities of swaged specimens with the respective oxides. Considerable difficulty was experienced in rolling the rods to area reductions comparable to those obtained by swaging. Rod diameters were reduced by 1/16-inch decrements, and several passes through each groove were usually required.

The maximum densities obtained in the rolled rods were 78% of theoretical for PWR-grade oxide and 89% of theoretical for fused uranium oxide; these compared with 75 and 93%, respectively, for swaged rods. The rolled PWR-grade oxide had a sheath of 0.145-inch-thick stainless steel, whereas the swaged rod had a 0.065-inch-thick cladding. The fused oxide specimen was preswaged from 0.750- to 0.688- inch diameter, then rolled to 0.530-inch diameter, at which stage it cracked.

The effects of sheath materials and dimensions on UO<sub>2</sub> densities in rolled rods were roughly analogous to the behavior observed in swaged rods. The data for rolled rods are much less extensive, however. Maximum densities obtained by various combinations of treatments and materials are listed and compared with swaging results in Table VII. The specimens sheathed in carbon steel reached slightly lower oxide densities than did those sheathed in stainless steel. A composite sheath, stainless steel within carbon steel, conferred no advantages.

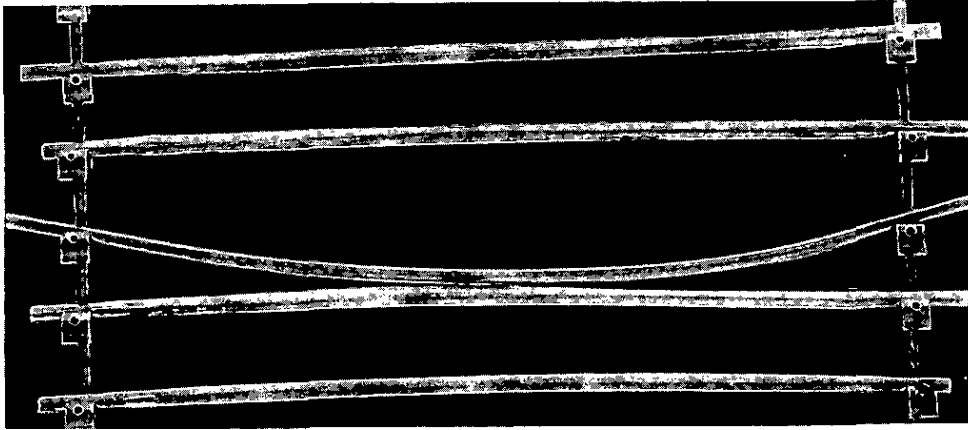
TABLE VII  
Density of UO<sub>2</sub> in Rolled Rods

Type of UO <sub>2</sub>	Sheath Dimensions, inch		Preswaged	Final Diameter, inch	Area Red'n, %	Final UO <sub>2</sub> Density, % of theo.	Density in a Comparable Swaged Rod, % of theo.	
	Material	Diameter						Wall Thickness
PWR Grade	Type 316 Stainless Steel	0.847	0.145	No	0.563 <sup>(a)</sup>	65	78	75
"	"	0.837	0.106	No	0.625 <sup>(a)</sup>	51	74	71
"	"	0.750	0.065	No	0.500	64	76	74
"	Carbon Steel	0.750	0.065	to 0.625	0.500 <sup>(a)</sup>	62	70	71
"	"	0.750	0.065	No	0.500	64	74	71
"	Composite: SS in CS	0.750	0.035	to 0.625	0.563 <sup>(a)</sup>	64	72	-
"	"	0.880	0.065					
Fused	Stainless Steel	0.750	0.035	to 0.688	0.530 <sup>(a)</sup>	48	89	91.5
"	"	0.750	0.035	No	0.625 <sup>(a)</sup>		(b)	-
"	Carbon Steel	0.750	0.065	No	0.563	46	86-88	-
"	"	0.750	0.065	No	0.500	60	88	-

<sup>(a)</sup> Cracked on final pass through rolls

<sup>(b)</sup> Failed too severely for density measurements

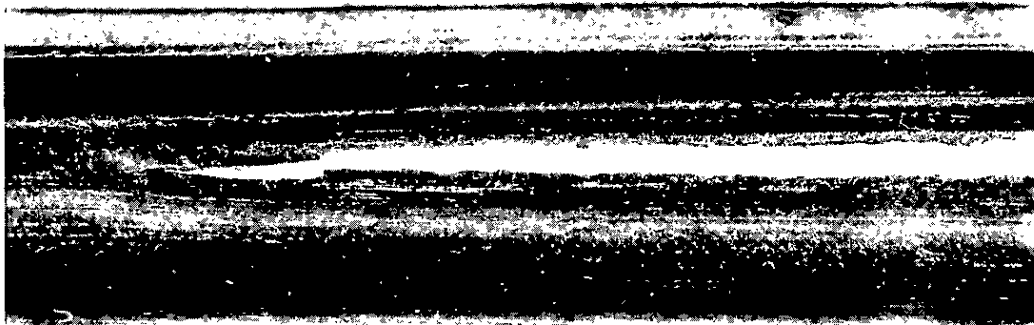
Many of the rods bowed, finned, and split during rolling. Of the first 25 rods rolled, 22 were cracked along the longitudinal direction. All rods exhibited severe finning, ovality, variations in wall thickness, and warp. A group of typical rolled rods is shown in Figure 16; a closeup of a split sheath appears in Figure 17.



Neg. 17353

Mag. 0.16X

FIGURE 16 - ROLLED ROD ELEMENTS  
 $\text{Al}_2\text{O}_3$  Clad in Stainless Steel

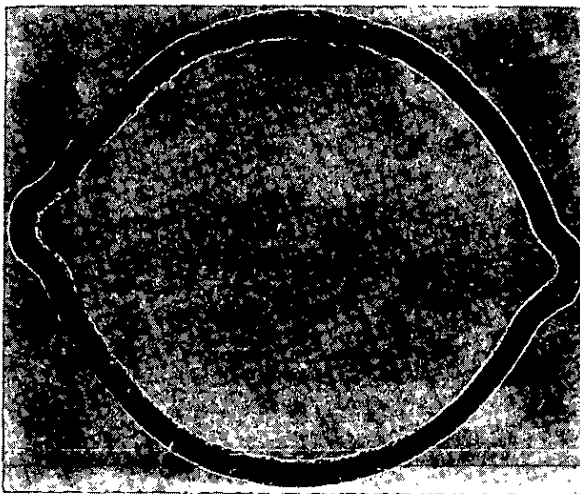


Neg. 20515

Mag. 3.4X

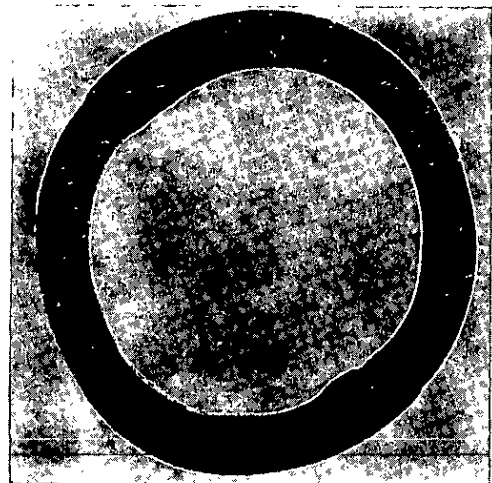
FIGURE 17 - SHEATH FAILURE OF A ROLLED ROD  
 $\text{Al}_2\text{O}_3$  Clad in Stainless Steel

Figure 18 shows cross sections of sheaths for 0.065- and 0.035-inch-wall specimens. The 0.035-inch-wall specimen shows the fins that were produced by the groove ovality and the roll parting, or relief space between the rolls. The 0.065-inch-wall specimen was rolled repeatedly through the same groove in an attempt to improve the external appearance. Even then the final shape was somewhat oval, and there was a thickening of the sheath in two places caused by the superficial removal of fins formed on a previous pass. A slight improvement was achieved with a composite sheath as shown in Figure 19; the outer sheath was finned severely, but the inner sheath was less so.



Neg. 17596

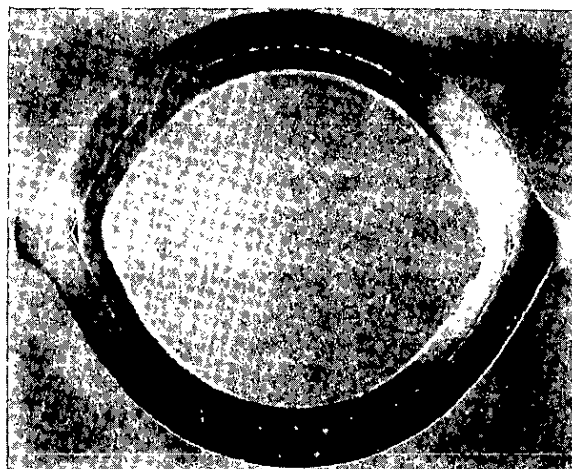
Mag. 4.25X



Neg. 17597

Mag. 4.25X

**FIGURE 18 - CROSS SECTIONS OF SWAGED-AND-ROLLED RODS**  
 Cross sections of sheaths from rod elements were formed by swaging followed by rolling. The core material has been removed and the sheaths mounted for inspection.



Neg. 18052

Mag. 3.25X

**FIGURE 19 - CROSS SECTION OF ROLLED ROD - COMPOSITE SHEATH**  
 Cross Section of a Rolled Rod with a Composite Sheath:  
 Carbon Steel Outer Sheath, Stainless Steel Inner Sheath

## ROLLING OF RIBBONS

Ribbon shapes were formed by loading uranium oxide into metal tubing and rolling it flat between plain rolls. The specimens were passed through the 16-inch-diameter rolls at a speed of 10 ft/min. Roll spacing was reduced by 0.050-inch decrements in the early stages of reduction, and by 0.025-inch decrements in the later stages.

The uranium oxide density in the rolled ribbons increased with area reduction more rapidly at low reductions than did similar swaged rods, but at high reductions the density was lower in comparison. Figure 20 illustrates this density behavior for PWR-grade oxide sheathed in Type 316 stainless steel; the density was still increasing slightly at the highest reduction obtained, 56%. Further reductions were prevented by specimen failures, usually over an end plug.

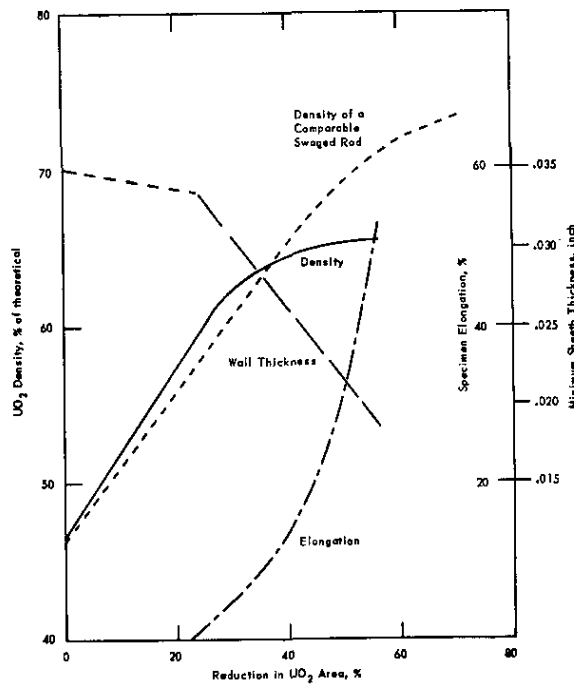


FIGURE 20 - ROLLING BEHAVIOR OF RIBBONS - PWR-GRADE UO<sub>2</sub>  
Type 316 Stainless Steel Cladding; Initial Rod  
Diameter = 0.750 inch, Wall Thickness = 0.035 inch

Rolled ribbons of PWR-grade uranium oxide in stainless steel sheathing reached higher final densities when preswaged in rod form than when not preswaged, but in neither case were the densities as high as for rods swaged to an equivalent area reduction.

Specimens initially 3/4 inch in diameter with an 0.035-inch sheath thickness reached a density of 65.5% of theoretical when flat-rolled to an area reduction of 56%, but reached 71% of theoretical when swaged through the same area reduction in rod form. A specimen roll-flattened to a total reduction of 56% after being preswaged through

a 46% area reduction in rod form reached a density of 69%, intermediate between those rolled only and those swaged only. A slight increase in final density was obtained by preswaging the end portions of the specimens before rolling them flat; this increase was about 1% of theoretical, half that given by preswaging the entire specimen. Whether the end plugs were rubber or metal backed by rubber did not affect the density. Specimens preswaged in rod form and then rolled flat have, of course, different final dimensions in cross section than specimens rolled to the same total area reduction without preswaging.

Ribbons of fused  $UO_2$  in stainless steel were rolled to a maximum oxide density of 86.5% of theoretical, which was about 5% less than the density normally reached in swaged rods of similar material. Reductions beyond 40% caused a decrease in oxide density, as shown in Figure 21.

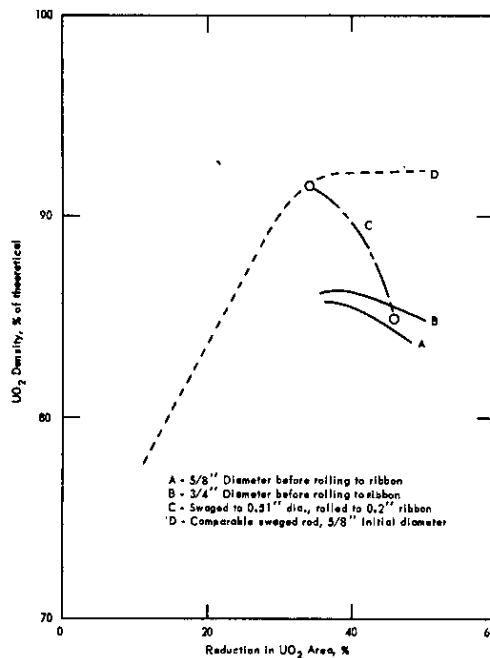
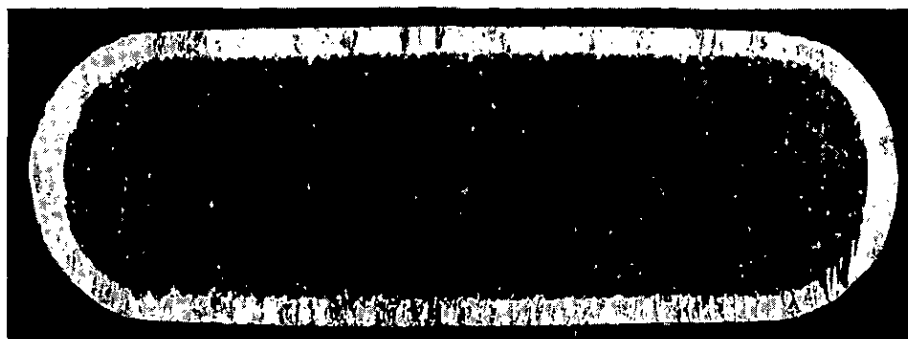


FIGURE 21 - ROLLING BEHAVIOR OF RIBBONS - FUSED  $UO_2$   
 Minus 20-Mesh, Grade 2, Fused  $UO_2$ , Sheathed in Type 316 Stainless Steel

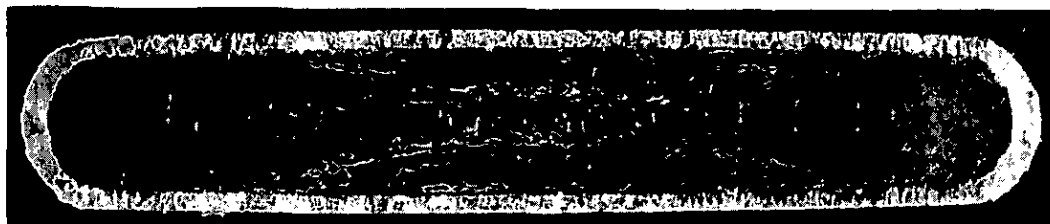
A specimen swaged to a density of 91% of theoretical at an area reduction of 36%, and then flattened by rolling, suffered a density decrease to 84% of theoretical, even though the total area reduction had increased to 47%. During flattening from a rod of 0.51-inch diameter to a ribbon only 0.2 inch thick, the sheath thickness was reduced from 0.034 to 0.019 inch at the thinnest point, the center of the flat face. The decrease in density probably resulted from small voids induced by the forced flow of the oxide and from the effect of sheath springback. There were no appreciable differences in final density between rolled ribbons with preswaged ends and those without preswaged ends for the specimens containing the fused oxide. A straticulate structure appeared in the oxide at about 30% area reduction. Figure 22 shows the stratification in the cross sections of two rolled ribbons; the onset of the phenomenon is just detectable in the upper photograph (area reduction 31%, thickness 0.34 inch), but is quite pronounced in the lower one (area reduction 52%, thickness 0.205 inch). Several changes in behavior occur at approximately 30% area reduction; the most significant, perhaps, is the rapid change in slope of the curve of density versus area reduction. At a slightly lower reduction, about 25%, wall thinning and specimen elongation first become appreciable (see Figure 20); these indicate, respectively, the increasing resistance of the oxide to further densification and the onset of lengthwise flow of the powder. Relevant data are given in Table VIII.



Neg. 18049

Mag. 4.25X

a.  $UO_2$  Density = 65% of Theoretical  
 $UO_2$  Area Reduction = 31%



Neg. 18050

Mag. 4.25X

b.  $UO_2$  Density = 69% of Theoretical  
 $UO_2$  Area Reduction = 52%

FIGURE 22 - CROSS SECTIONS OF ROLLED RIBBONS  
 PWR-Grade  $UO_2$  in Type 316 Stainless Steel Rolled Flat  
 from Rod Shapes Initially 3/4 Inch in Outside Diameter

TABLE VIII

Stratification in Flat-Rolled Specimens

PWR-grade UO<sub>2</sub> in Type 316 stainless steel  
 Initial diameter = 0.750 inch  
 Initial wall thickness = 0.035 inch

Area Reduction, %	Rate of Change of Density <sup>(a)</sup>	Ribbon Thickness, inch	Sheath Thickness, <sup>(b)</sup> inch	Specimen Elongation, %	Stratificate Structure
25	0.53	0.39	0.034	0	None
30	0.37	0.34	0.030	7	Slight
38	0.18	0.29	0.028	10	Yes
47	0.08	0.24	0.022	25	Yes
51	0.06	0.21	0.021	35	Pronounced
56	0.05	0.18	0.019	52	Pronounced

(a) Slope =  $\frac{\Delta\% \text{ of theoretical}}{\Delta\% \text{ area reduction}}$

(b) Thickness at middle of the flattened portion

It is not certain whether the layer structure and the abrupt slope change of the density curve were caused by lengthwise movement of the powder or by springback of the sheath after rolling, but the latter is favored by the following consideration. Swaged rods have elongations comparable to rolled ribbons, but they do not exhibit the rapid change of slope in the density curve. Therefore, the basic difference between swaged rods and rolled ribbons may lie in the lesser sheath springback that is characteristic of the rod shape.

A slight effect of initial diameter on final density was observed. The smaller initial diameters gave higher final densities with PWR-grade uranium oxide (Figure 23), as was the case with swaged rods.

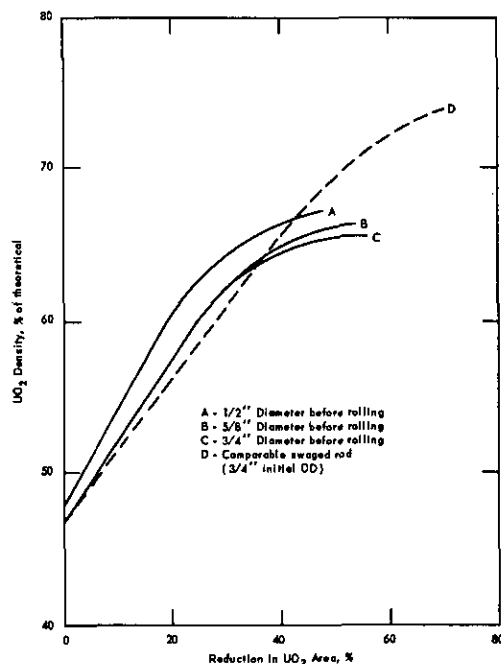
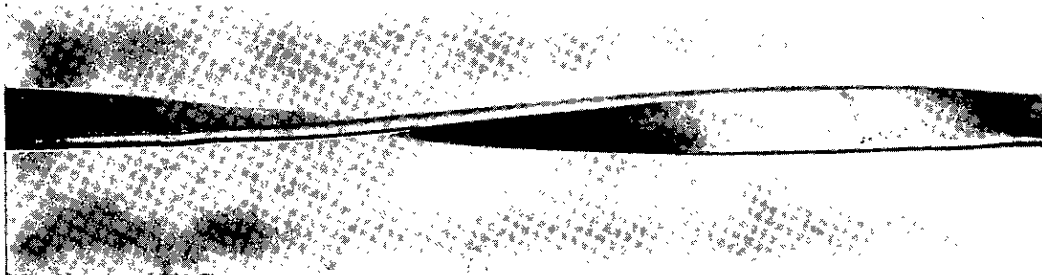


FIGURE 23 - EFFECT OF ROD DIAMETER ON UO<sub>2</sub> DENSITY IN ROLLED RIBBONS  
 PWR-Grade UO<sub>2</sub> in Type 316 Stainless Steel Tubing; Initial Wall Thickness = 0.035 Inch

The reverse appeared to be true for fused uranium oxide (Figure 21), but this may be because the specimens of 5/8-inch initial diameter had already passed their peak densities at the area reductions shown on the graph. No data were taken for area reductions less than 36.5%.

The ribbons tended to develop camber - bending in the plane of the ribbon - at the large area reductions, typically at reductions greater than 35%. Bow was seldom a problem.

The ribbons could be twisted after being annealed to restore ductility. Figure 24 shows a section of ribbon twisted through approximately 180 degrees per foot. Twisting without prior annealing required much more force and produced a very irregular pitch. The twisting was performed with a vise and a large wrench.



Neg. 18009

Mag. 0.44X

#### FIGURE 24 - TWISTED RIBBON ELEMENT

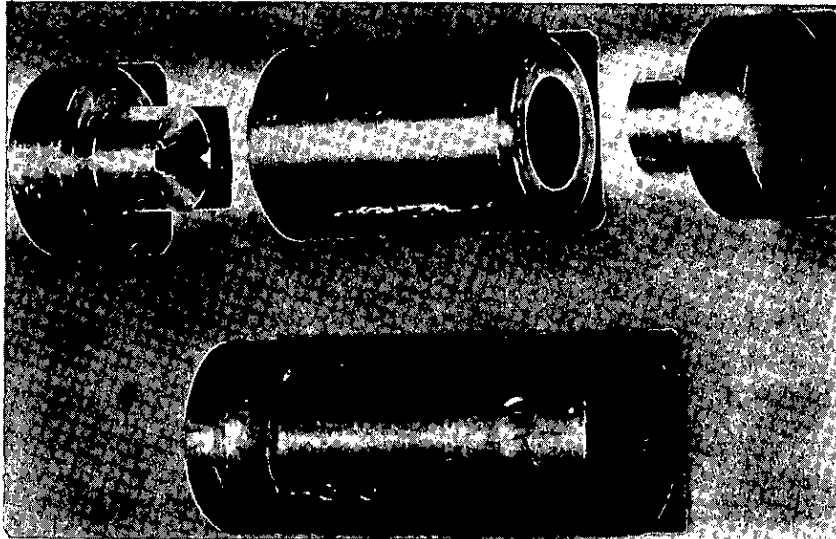
A Twisted Ribbon of PWR-Grade Oxide in Stainless Steel. The Specimen was Rolled Flat from a Rod Shape, Annealed, and Twisted in a Vise.

Uranium oxide densities within the twisted ribbons could not be measured accurately because the compacted oxide, being broken up by the twisting movement, was inadequately retained within the small sections that were cut for evaluation.

#### COEXTRUSION OF RODS

Experimental coextrusions were made of fused uranium oxide sheathed in aluminum. Aluminum sheaths were used to simplify the study of the low temperature extrusion behavior of  $UO_2$ , and not because Al cladding was desired in the final product. A consistently successful extrusion ratio was 6.6:1, which resulted in aluminum-clad oxide rods of 0.525-inch nominal diameter. The temperature of extrusion was 445 to 480°C. The billets were extruded at either 0.5 or 3 inches per minute with no apparent differences in the results; the force on the 1-3/8-inch-diameter ram was 55,000 pounds (a pressure of 37,000 lb/in<sup>2</sup>) at the beginning of the extrusion. The extrusion dies were of the streamline-flow type with a 90° included angle in the die cone. The extrusion assembly was a small experimental design that was intended

for use with a mechanical testing machine. Exploded and assembled views of the extrusion billets are shown in Figure 25, and typical as-extruded rods are shown in Figure 26.



Neg. 20508

Mag. 0.65X

FIGURE 25 - COEXTRUSION BILLETS  
Exploded and Assembled Views of Composite Billets  
for Coextrusion of  $UO_2$  in an Aluminum Alloy Sheath



Neg. 20507

Mag. 0.25X

a. Over-all View



Neg. 18380

Mag. 1.1X

b. Close-up View

FIGURE 26 - TYPICAL COEXTRUDED RODS  
Typical As-Extruded Rods. Fused  $UO_2$  Clad in Aluminum Alloy

The final densities of the uranium oxide were low compared to those obtained by swaging or rolling of fused oxide. The initial and final densities of several specimens, together with the particle sizes of the oxide, are given in Table IX. The larger particle sizes produced higher densities, but they also caused greater roughening of the inner surface of the cladding.

TABLE IX

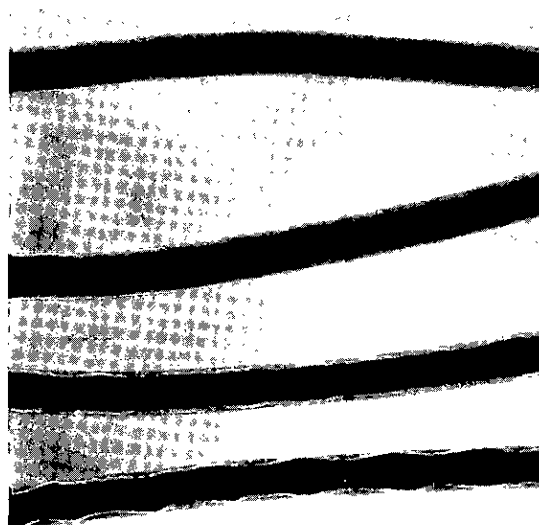
Density of UO<sub>2</sub> in Coextruded Rods

Sieve Size of UO <sub>2</sub> <sup>(a)</sup>	Density, % of theoretical	
	Initial	Final
-16	52.3	75.8
-20	50.3	72.9
-40	52.3	70.9
-120	49.1	71.2
-200	44.0	69.2

(a) All particles that passed the sieve number listed (U. S. Standard Sieve Sizes) were used.

A temperature high enough to give some plastic deformation of the oxide, 800°C or above, <sup>(15)</sup> would probably be required to achieve a high oxide density by means of coextrusion.

Sheath thickness exhibited a cyclic variation along the rod length as well as minor variations at a given cross section. A radiograph of four extruded rods is shown in Figure 27, and a cross-section of a rod is shown in Figure 28.

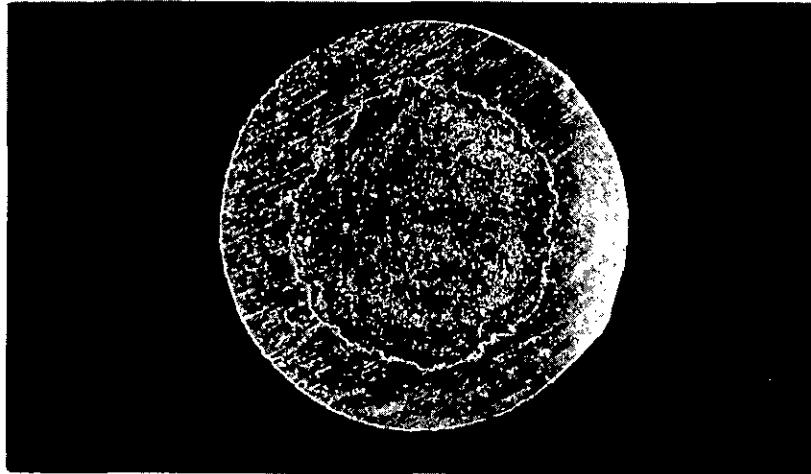


Film No. 707 D

Mag. 0.5X

FIGURE 27 - RADIOGRAPHS OF COEXTRUDED RODS  
Fused UO<sub>2</sub> Clad in Aluminum Alloy

The sheath thicknesses of the extruded rods varied from 0.14 to 0.17 inch, and the outside diameter varied from 0.50 to 0.52 inch. The nonuniformities in the core and sheath were probably caused by a pulsating flow of the  $UO_2$  powder through the die. During the minima of the oxide flow the aluminum sheathing moved in to fill the deficiency in the core, causing the sheath to vary in thickness.



Neg. 20513

Mag. 4.2X

FIGURE 28 - CROSS SECTION OF COEXTRUDED ROD  
Fused  $UO_2$  Clad in Aluminum Alloy

Aluminum alloys employed as cladding materials included Types 1100, 5052, and 5154. Rods clad with the harder alloys, 5052 and 5154, had better surfaces and smaller core end defects than did rods clad with 1100 aluminum.

Attempts to extrude with extrusion ratios of 15:1 and 10:1 resulted in failure of the extrusion assembly. In a failure at a 15:1 extrusion ratio the uranium oxide reached a density of 90% of theoretical in the unextruded part of the billet but only 75% in the extruded portion. In such cases, the force on the ram increased during the course of the extrusion until the failure occurred. The ram force decreased slightly during the successful extrusion at a ratio of 6.6:1.

*G. R. Cole*  
G. R. Cole

*A. S. Ferrara*  
A. S. Ferrara

*H. H. Kranzlein*  
H. H. Kranzlein  
Pile Materials Division

## BIBLIOGRAPHY

1. Eichenberg, J. D., et al., Effects of Irradiation on Bulk Uranium Dioxide, Westinghouse Electric Corp., WAPD-183, October 1957. (TID-7546, pp. 442-515)
2. Robertson, J. A. L., et al., "Behavior of Uranium Oxide as a Reactor Fuel", Proc. U. N. Intern. Conf. Peaceful Uses Atomic Energy, 2nd, Geneva, 1958, 6, 655-76 (1958). P/193
3. Materials for Nuclear Reactors, Bernard Kopelman, ed. New York: McGraw Hill (1959).
4. Aronson, S., "Oxidation of  $UO_2$  in Water Containing Oxygen". Bettis Technical Review. Reactor Metallurgy, Westinghouse Electric Corp., WAPD-BT-10, pp. 93-5, October 1958.
5. Kingery, W. D., et al., "Thermal Conductivity: X, Data for Several Pure Oxide Materials Corrected to Zero Porosity". J. Am. Ceram. Soc. 37, 107 (1954).
6. Hedge, J. C., Measurement of Thermal Conductivity of Uranium Oxide, Illinois Institute of Technology, Chicago, Armour Research Foundation, AECU-3381, September 1956.
7. Scott, R., Thermal Conductivity of  $UO_2$ , Atomic Energy Research Establishment, Harwell, Berks., AERE M/R 2526, March 1958.
8. Ross, A. M., A Literature Survey on the Measurement of Thermal Conductivity of Several Solids Including Uranium Dioxide, Atomic Energy of Canada, Ltd., CRFD-762, March 1958.
9. Stenquist, D. R. and Anicetti, R. J., "Fabrication of Ceramic Fuel Elements by Swaging". Nuclear Metallurgy 5, Symposium on the Fabrication of Fuel Elements (1958).  
  
Also the periodic reports from the Hanford Atomic Products Operation of the General Electric Company.
10. Patterson, D. L. and Chalder, G. H., The Integral Fabrication of Uranium Dioxide Fuel Elements by Rotary Swaging, Atomic Energy of Canada, Ltd., CRFD-759, June 1959.  
  
Also the periodic reports from the Chalk River Laboratory of Atomic Energy of Canada, Ltd.
11. Clayton, J. C. and Aronson, S., "Densities of Uranium Oxide in the Region  $UO_2-U_4O_9$ ". Bettis Technical Review. Reactor Metallurgy, Westinghouse Electrical Corp., WAPD-BT-10, pp. 96-100, October 1958.
12. Stenquist, D. R., Hanford Atomic Products Operation. Private Communication.

13. Scott, R., The Warm-Pressing (800°C) of Uranium Dioxide and Uranium Dioxide - Metal Mixtures, Atomic Energy Research Establishment, Harwell, Berks., AERE M/R-2396. September 1957.
14. Belle, J. and Lustman, B., Properties of Uranium Dioxide, Westinghouse Electric Corp., WAPD-184, September 1957. (TID-7546, pp. 616-716).
15. Hall, A. R., Scott, R., and Williams, J., The Plastic Deformation of Uranium Oxides Above 800°C, Atomic Energy Research Establishment, Harwell, Berks., AERE M/R-2648, August 1958.